ARTICLE NO. 79-0294R

Interaction of Two Burning Fuel Droplets of Arbitrary Size

T.A. Brzustowski* and E.M. Twardus†
University of Waterloo, Waterloo, Ontario, Canada
and
S. Wojcicki‡ and A. Sobiesiak§
Technical University of Warsaw, Warsaw, Poland

The combustion of two interacting droplets of arbitrary size was analyzed by solving Laplace's equation in bispherical coordinates, with the conjecture that multiplication by $\ell n(1+B)$ converts the diffusion rate in the absence of a flame to the evaporation rate of a burning droplet. Closed-form solutions were obtained both for the burning rate of each droplet and for the shape of the flame. The burning rate of each droplet was found to be smaller than that of an isolated droplet of the same size. The reduction was greatest when the droplets were touching, and was relatively larger for the smaller droplet. Two simple functions, one for the larger droplet and one for the smaller, were found to give good approximations to the burning rate of touching droplets. Free-fall experiments were performed to check the theory. The results available so far have provided qualitative support for the mathematical model in that observed flames of some pairs of burning droplets strongly resemble the calculated flame shape.

Nomenclature

a = parameter of bispherical coordinates
a/f = stoichiometric air/fuel ratio by weight
dA_η = area element in surface η = constant
B = $[c_p(T_\infty - T_O) + (f/a)\Delta H_c Y_{ox,\infty}]/L_v$ transfer number for combustion
c_P = specific heat at constant pressure
$\mathfrak{D}$ = diffusion coefficient
f = function defined by Eq. (8)
g_1, g_2, g_3 = metric coefficients in bispherical coordinates
h = distance between the center of a drop and the origin of coordinates
ΔH_c = heat of combustion per unit mass of fuel
L_v = latent heat of evaporation
$\dot{m}$ = evaporation or burning rate
p = separation constant
P_p = Legendre polynomial
R = resistance to heat transfer or diffusion
r_f = flame radius
r = droplet radius
T_O = droplet surface temperature
T_∞ = ambient gas temperature
W = molecular weight
Y_F = mass fraction of diffusing fuel vapor
$Y_{F,O}$ = mass fraction of fuel vapor at droplet surface
Y_{ox} = mass fraction of oxygen
$Y_{ox,\infty}$ = mass fraction of oxygen in ambient air
β' = passive scalar
η, θ, ψ = bispherical coordinates
ν = stoichiometric coefficient
ρ = density
ϕ = $\dot{m}(h_1+h_2)/\dot{m}(\infty)$ reduced burning rate
ϕ_t = $\dot{m}(r_1+r_2)/\dot{m}(\infty)$ reduced burning rate when droplets touch
ϕ_t^* = approximation to ϕ_t

Subscripts

1 = larger droplet
2 = smaller droplet
t = at tangency

Presented as Paper 79-0294 at the AIAA 17th Aerospace Sciences Meeting, New Orleans, La., Jan. 15-17, 1979; submitted Jan. 23, 1979; revision received May 18, 1979.

Index category: Combustion and Combustor Designs.

*Professor, Dept. of Mechanical Engineering. Member AIAA.
†Research Associate, Dept. of Mechanical Engineering.
‡Professor, Faculty of Power and Aeronautical Engineering.
§Ph.D. Candidate, Institute of Heat Technology.

Introduction

THE concern with flame-generated pollutants in the combustion of liquid fuels has produced a revival of interest in the interactions between burning droplets.[1] Recent theoretical studies on this topic include those by Labowsky and Rosner,[2] Chiu and Liu,[3] Twardus and Brzustowski,[4] and Labowsky.[5] Experimental work on the interaction of droplets burning in falling arrays has been published by Twardus and Brzustowski[6] and by Sangiovanni and Dodge.[7]

The theoretical studies have been of two types: those in which the problem is reduced to the solution of Laplace's equation in the appropriate geometry[2,4] and those in which the burning behavior of a group of droplets is synthesized from the combustion characteristics of individual droplets by the application of appropriate integral theorems.[3] The transformation recently published by Labowsky[5] makes it possible to reduce the governing transport equations for a rapidly evaporating droplet to Laplace's equation. This useful result makes the many methods of potential theory more widely applicable in the evaporation and combustion of droplets.

In their earlier theoretical paper,[4] the authors from Waterloo used the bispherical coordinate system[8] to calculate the burning rate and the shape of the flame for two droplets of equal size. The use of such coordinate systems in problems of heat transfer has been advocated by Yovanovich,[9,10] whose work has shown their usefulness and made them accessible to thermal engineers.

The effect of separation between equal droplets on their burning rate is less dramatic than on the appearance of the flame. The burning rate is lowest when the drops are touching. At that condition the droplets burn with a single, nearly spherical flame and $\dot{m}(2h)$ is $\ell n\, 2$ (i.e., 0.693) times the burning rate of the individual droplet $\dot{m}(\infty)$. The burning

rate increases monotonically with increasing interdroplet distance. At a spacing of 8.5 diam, when the flame enveloping the droplets is close to separating into two distinct flames, the burning rate is already close to 90% of the single droplet rate. At a spacing of 20 diam, when the droplets burn with individual, nearly spherical flames, it is over 95%. The same result was obtained independently by Samson and Deutch,[11] who, in addition, showed that a useful approximation is $\dot{m}(2h)/\dot{m}(\infty) \simeq [1+(r/2h)]^{-1}$.

It should be pointed out that the results of Twardus and Brzustowski[4] were derived for a model in which the transport equations reduced to Laplace's equation. This means that the same results can be applied to conduction heat transfer, in which the ratio of resistances would be the same as $\dot{m}(\infty)/\dot{m}(2h)$.

In the present paper, the first two authors have extended the theory to the case of droplets of unequal size, and the last two authors have provided a qualitative verification of predicted flame shapes in free-fall experiments.

Mathematical Model

The analysis begins with the solution of Laplace's equation in the mass fraction of fuel Y_F. This solution yields the mass transfer rate from each droplet by quasisteady diffusion in a field with uniform properties, in the absence of convection and gravity.

The two droplets are represented by spheres of radii r_i and r_2 with their centers located a distance h_1+h_2 apart. The center of a bispherical coordinate system is located between the droplets, a distance h_1 from the center of sphere 1. Details of the bispherical coordinate system and of Laplace's equation in that system are given by Moon and Spencer.[8]

Laplace's equation takes the form

$$\frac{(\cosh\eta-\cos\theta)^3}{a^2\sin\theta}\left\{\sin\theta\frac{\partial}{\partial\eta}\left(\frac{1}{\cosh\eta-\cos\theta}\frac{\partial Y_F}{\partial\eta}\right)\right.$$

$$\left.+\frac{\partial}{\partial\theta}\left(\frac{\sin\theta}{\cosh\eta-\cos\theta}\frac{\partial Y_F}{\partial\theta}\right)\right\}+\frac{(\cosh\eta-\cos\theta)^2}{a^2\sin^2\theta}\frac{\partial^2 Y_F}{\partial\psi^2}=0 \quad (1)$$

with the boundary conditions: on droplet 1:

$$Y_F=Y_{F,O} \quad \text{at} \quad \eta=\eta_1$$

and on droplet 2:

$$Y_F=Y_{F,O} \quad \text{at} \quad \eta=-\eta_2$$

Also by symmetry:

$$\frac{\partial Y_F}{\partial\theta}=0 \text{ at } \theta=0 \text{ and } \theta=\pi, \quad \frac{\partial Y_F}{\partial\psi}=0 \text{ at } \psi=0 \text{ and } \psi=\pi$$

Y_F also automatically satisfies the boundary condition $Y_F=0$ at $\eta=\theta=0$, i.e., at an infinite distance from the two droplets.

The radii of the spheres are related to the distance h by the relations

$$h_1=r_1\cosh\eta_1, \qquad h_2=r_2\cosh\eta_2 \quad (2)$$

Composition Field

When the boundary conditions are applied and the orthogonality property of Legendre polynomials is used to evaluate the coefficients,[12] the final solution for the composition field surrounding two droplets takes the form

$$Y_F(\eta,\theta)=\sqrt{2}Y_{F,O}(\cosh\eta-\cos\theta)^{1/2}$$

$$\times\sum_{p=0}^{\infty}\left\{\frac{e^{-(p+1/2)(2\eta_1-\eta_2)}-e^{-(p+1/2)(\eta_2+\eta_1)}}{e^{(p+1/2)\eta_2}-e^{-(p+1/2)(2\eta_1+\eta_2)}}e^{-(p+1/2)\eta}\right.$$

$$\left.+\frac{e^{-(p+1/2)\eta_2}-e^{-(p+1/2)(2\eta_1+\eta_2)}}{e^{(p+1/2)\eta_2}-e^{-(p+1/2)(2\eta_1+\eta_2)}}e^{-(p+1/2)\eta}\right\}P_p(\cos\theta) \quad (3)$$

In the case of equal droplets, this reduces to the result published as Eq. (5) of Ref. 4.

Mass Transfer

The rate of mass transfer by diffusion from the droplets is given by

$$\dot{m}_1=\int\int_{A_1}\rho\mathfrak{D}(\text{grad}_\eta Y)\,dA_\eta \quad (4)$$

and

$$\dot{m}_2=-\int\int_{A_2}\rho\mathfrak{D}(\text{grad } Y)\,dA_\eta \quad (5)$$

where

$$\text{grad}_\eta Y=\frac{1}{\sqrt{g_1}}\frac{\partial Y}{\partial\eta} \quad \text{and} \quad dA_\eta=\sqrt{g_1g_2}\,d\theta d\psi \quad (6)$$

In these expressions, g_1, g_2, and g_3 are the metric coefficients of the bispherical coordinate system

$$g_1=g_2=\frac{a^2}{(\cosh\eta-\cos\theta)^2} \quad \text{and} \quad g_3=\frac{a^2\sin^2\theta}{(\cosh\eta-\cos\theta)^2} \quad (7)$$

The quantity a is a constant parameter of the coordinate system, given by $a=r_1\sinh\eta_1=r_2\sinh\eta_2$.

The droplet labeled 1 is in that half of the coordinate system (i.e., $0<\eta<\infty$) where successively larger spheres are represented by decreasing positive values of η. In that case, the outward normal from a sphere is in the direction of decreasing η, and there is no minus sign in the equation for the diffusion rate. Droplet 2 lies in the other half (i.e., $-\infty<\eta<0$, where successively larger spheres are represented by increasing negative value of η, and the minus sign is required in the equation for $\dot{m}$.

Since $Y_F(\eta,\theta)$ is now given by Eq. (3), $(\text{grad}_\eta Y)$ can be derived and $\dot{m}_1$ and $\dot{m}_2$ can be evaluated. Some tedious manipulation leads to the following results for the two diffusion rates:

$$\dot{m}_1^*=4\pi r_1\rho\mathfrak{D}Y_{F,O}\sinh\eta_1$$

$$\times\sum_{p=0}^{\infty}\left\{\frac{1}{\sinh 1/2[(2p+1)(\eta_1+\eta_2)+\eta_1-\eta_2]}\right.$$

$$\left.-\frac{1}{\sinh 1/2[(2p+2)(\eta_1+\eta_2)]}\right\}=4\pi r_1\rho\mathfrak{D}Y_{F,O}f(\eta_1,\eta_2) \quad (8)$$

$$\dot{m}_2^*=4\pi r_2\rho\mathfrak{D}Y_{F,O}f(\eta_2,\eta_1) \quad (9)$$

where the function $f(\eta_1,\eta_2)$ is defined by Eq. (8) and the asterisk identifies the slow diffusion rate.

Burning Rates

The mass transfer rate derived from the solution of Laplace's equation applies to the process of slow diffusion from a source into a stagnant medium with a sink at infinity. Without any further modification, these results could be used to calculate the evaporation rates and the composition field of two droplets of fuel in a cold gas.

However, the burning of a droplet differs from this process in two ways: the chemical reaction which consumes the fuel provides a sink for the vapor in the vicinity of the drop, and the evaporation rate is so fast that it induces a bulk convection of the vapor away from the droplet surface (Stefan flow). The classical theory of droplet combustion[13] takes both these effects into account. A convective term in the equations of conservation of molecular species and the appropriate boundary condition at the droplet surface account for Stefan flow. The chemical reaction is dealt with on the assumption that reaction rates vastly exceed transport rates. Combustion is thus portrayed as taking place in a thin flame sheet where fuel vapor and oxygen meet in stoichiometric proportions. The additional assumption that $\lambda/c_P=\rho\mathfrak{D}$ (i.e., that the Lewis number is 1) allows the composition and temperature fields to be treated as similar.

In the case of a single droplet of radius r burning in an infinite stagnant oxidizing gas, quasisteady theory gives the well-known result

$$\dot{m}=4\pi r\rho\mathfrak{D}\ell n(1+B) \tag{10}$$

where B is the transfer number.[13] The same equation describes the rate of evaporation into hot gas, with the difference that B for evaporation does not contain the term involving the heat of combustion.

The rate of mass transfer by diffusion from a single spherical source into an infinite stagnant gas is:

$$\dot{m}=4\pi r\rho\mathfrak{D} \tag{11}$$

on the assumption, in this case, that the mass fraction of vapor at the surface is 1. On this basis, the conjecture was advanced in Ref. 4 that multiplication by $\ell n(1+B)$ would convert diffusion rates to burning rates. Subsequently, Labowsky[5] has shown that the mass average velocity applicable to the fast evaporation of a droplet into an inert substance (i.e., in the case when Stefan flow occurs) is given by $-\mathfrak{D}\omega_0\ell n(1+B)\nabla\omega$, where ω is a variable which satisfies $\nabla^2\omega=0$ with the boundary conditions $\omega=\omega_0$ on the surface of the droplet and $\omega=0$ at infinity. This result leads to the expression for the fast evaporation rate, or burning rate if the transfer number B is appropriately defined.

Therefore, it is proposed that the burning rates of the two droplets are:

$$\dot{m}_1=4\pi r_1\rho\mathfrak{D}\ell n(1+B)f(\eta_1,\eta_2) \tag{12}$$

$$\dot{m}_2=4\pi r_2\rho\mathfrak{D}\ell n(1+B)f(\eta_2,\eta_1) \tag{13}$$

In the case of two droplets of equal size, Eqs. (12) and (13) both reduce to the result published in Ref. 4.

Flame Shape

The approach taken to calculate the shape of the flame is the same as that in Ref. 4. The passive scalar,

$$\beta'\equiv(Y_F/W_F\nu_F)-(Y_{ox}/W_{ox}\nu_{ox})+Y_{ox,\infty}/W_{ox}\nu_{ox})$$

takes a constant value at the surface of the droplets and zero at infinity. The thin flame sheet is the surface given by $\beta'=(Y_{ox,\infty}/W_{ox}\nu_{ox})$. The equation relating η and θ on the flame sheet is Eq. (3), with $Y_F(\eta,\theta)$ replaced by $(Y_{ox,\infty}/W_{ox}\nu_{ox})$ and $Y_{F,O}$ replaced by $(Y_{F,O}/W_F\nu_F)+(Y_{ox,\infty}/W_{ox}\nu_{ox})$.

In the case of an isolated droplet, this approach gives[4]

$$\frac{r_f}{r}=1+\frac{(Y_{F,O}/W_F\nu_F)}{(Y_{ox,\infty}/W_{ox}\nu_{ox})}=1+\frac{a}{f} \tag{14}$$

where a/f is the stoichiometric air-fuel ratio by weight. This result should be compared with the result of quasisteady theory[13]

$$\frac{r_f}{r}=\frac{\ell n(1+B)}{\ell n\left\{1+\dfrac{(Y_{ox,\infty}/W_{ox}\nu_{ox})}{(Y_{F,O}/W_F\nu_F)}\right\}}=\frac{\ell n(1+B)}{\ell n(1+f/a)} \tag{15}$$

For hydrocarbons such as heptane and octane burning in air, the air/fuel ratio is about 15, so that Eq. (14) gives r_f/r of about 16. For the same condition Eq. (15) gives r_f/r of about 15.5 $\ell n(1+B)$. The correction for Stefan flow again seems to be $\ell n(1+B)$, a number of order 2 for hydrocarbons burning in air.[14] This correction is evident, since for $(a/f)\gg 1$, Eq. (15) reduces to $(a/f)\ell n(1+B)$.

The quasisteady prediction of flame size is not as certain as the quasisteady prediction of burning rate. There are few experiments in which predicted and measured flame radii are compared, and the few that there are[15-17] suggest that quasisteady theory with constant properties significantly overestimates the flame radius. For this reason, no attempt is made in the present work to correct the predicted flame radius for Stefan flow.

Theoretical Results

Burning Rates

An obvious result of the theory is that the burning rate of each droplet is proportional to its radius, just as in the case of the isolated droplet. This means that the "d^2 law" still applies. It also means that the ratio of the two radii will increase with time as the droplets burn.

It is clear that the interaction of two droplets decreases the burning rate of each. The variation of burning rate with distance between drops is shown in Fig. 1. The three curves in the figure show the burning rate of the smaller droplet, the burning rate of the larger droplet, both for $r_1/r_2=6$, and the burning rate of each of a pair of equal droplets. In each case, the burning rate is nondimensionalized by the burning rate of the same droplet in isolation. Thus, $\phi_1\equiv\dot{m}_1(h_1+h_2)/\dot{m}_1(\infty)$ and $\phi_2\equiv\dot{m}_2(h_1+h_2)/\dot{m}_2(\infty)$. The burning rate of the smaller droplet decreases monotonically as the droplets are placed closer together with the minimum burning rate when they are touching. The burning rate of the bigger droplet varies far less, but not entirely monotonically. For $r_1/r_2>3$, it is minimum not at tangency but at h_1+h_2 slightly less than 2 r_1/r_2. The minimum value is about 1% smaller than the value at tangency.

The relative reduction of the burning rate is greater for the smaller droplet. This effect increases with increasing ratio of

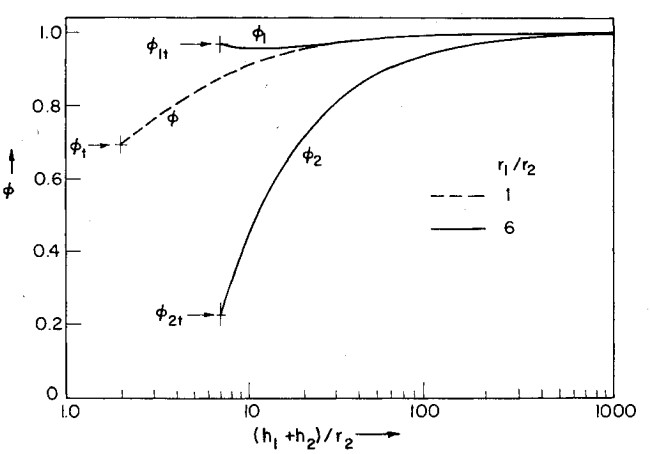

Fig. 1 Variation of reduced burning rate ϕ with distance between droplet centers (h_1+h_2) for equal droplets (dashed line, $r_1/r_2=1$) and unequal droplets (solid line, $r_1/r_2=6$).

Table 1 Relative reduction of the burning rates for touching droplets—exact results and approximate functions

r_1/r_2	ϕ_1	ϕ_1^*	ϕ_2	ϕ_2^*
1	0.6931	0.488	0.6931	0.800
2	0.852	0.808	0.494	0.533
3	0.912	0.898	0.381	0.400
4	0.942	0.936	0.310	0.320
5	0.959	0.956	0.261	0.267
6	0.970	0.968	0.226	0.229
7	0.976	0.976	0.198	0.200
8	0.981	0.981	0.177	0.178
9	0.984	0.984	0.160	0.160
10	0.987	0.987	0.146	0.146
15		0.994	0.100	0.100
20		0.996	0.077	0.076
∞		1		0

droplet sizes, and is most pronounced when the droplets are in contact. The results are shown in Table 1. The quantity $\phi_{1_t} \equiv \dot{m}_1(r_1+r_2)/\dot{m}_1(\infty)$ is the ratio of the burning rate of the larger droplet at tangency to the burning rate of the same droplet in isolation. $\phi_{2_t} \equiv \dot{m}_2(r_1+r_2)/\dot{m}_2(\infty)$ is the corresponding quantity for the smaller droplet. All of the values listed except the first are extrapolations of computed results. The value 0.6931 is $\ell n\ 2$, the result obtained analytically for equal droplets.[4]

The functions $\phi_{1_t}^* = 1 - [1.536\, r_2^2/(r_1^2+2r_1r_2)]$ and $\phi_{2_t}^* = 1.6\, r_2/(r_1+r_2)$ are useful approximations to ϕ_{1_t} and ϕ_{2_t}, respectively, for large ratios of the radii where computation is difficult.

Flame Shape

The computed flame shapes are shown in Figs. 2-5. For each radius ratio, the effect of increasing the spacing between droplets is qualitatively the same. When the droplets are close together, a single, nearly spherical flame envelops them both. As spacing is increased, the single flame becomes increasingly distorted and eventually separates into two flames which, in turn, become more nearly spherical as the droplets are moved far apart.

It is shown in Ref. 4 that two equal droplets burn with separate flames, provided their centers are more than 17.067 diam apart. This result was interpreted in terms of a cone. If that same cone describes the relative location of unequal droplets at the point when their flames separate, the quantity h_1+h_2 at separation should be proportional to r_1+r_2.

Even though it is difficult to compute precisely the value of h_1+h_2 at separation, the bounds on that quantity make it quite clear that residence within a single cone is not the criterion for flame separation for droplets of all sizes. When r_1/r_2 is large, the flames separate when the droplets are closer together than the cone criterion would suggest, i.e., at $(h_1+h_2)/r_2$ of about 130 rather than 196 for $r_1/r_2=20$. The approximate droplet spacing at which the flames separate is listed in Table 2.

Implications for Conduction Heat Transfer

The resistance to heat transfer between two spherical particles at the same uniform temperature and a heat sink at infinity is inversely proportional to $\dot{m}$. Therefore, $R_1(h_1+h_2)/R_1(\infty) = 1/\phi_1$, and in the limit of touching spheres, $R_1(r_1+r_2)/R_1(\infty) = 1/\phi_{1_t}$. This means that the presence of a large particle in proximity to a small one at the same temperature renders the small particle more nearly adiabatic. The effect of an adiabatic wall in contact with the spherical particle is given by the value of ϕ_t for $r_1/r_2=1$. In this case, the thermal resistance increases by a factor of $1/\ell n 2$, or some 44%.

Table 2 Relative spacing of droplets for flame separation

r_1/r_2	$(h_1+h_2)/r_2$
1	17.067
2	~25
4	~40
6	~53
10	~73
15	~104
20	~130

This particular result may be of considerable importance in the initiation of dust explosions. Dust particles undergoing an exothermic reaction-rate limited surface oxidation are more nearly adiabatic when they are close together than they would be as isolated particles. This effect may be particularly pronounced when dust particles lie on a warm, nonconducting solid object of large dimensions, such as a concrete ledge or a wooden beam. In such circumstances, and given the relatively small temperature increase which might be sufficient for ignition, the large object could act more as an isothermal surface at the same temperature than as an adiabatic one. This would mean that the rate of heat loss from the particle to the ambient gas could decrease by far more than 44%.

Experimental Study

The experimental phase of this work was performed in a 10-m free-fall facility at the Institute of Heat Technology of the Technical University of Warsaw (see Fig. 6). The initial results of these experiments provide strong qualitative support for the prediction of flame shapes discussed previously.

The experimental apparatus is an adaptation of the one used by Kumagai.[15] Two droplets are suspended on thin filaments in air at 1 atm. At time $t=0$, the filaments are rapidly withdrawn, the apparatus is dropped, and a spark is discharged in the vicinity of one droplet. As the experiment progresses, the flame is photographed by a camera mounted on the falling platform.

To overcome the aerodynamic resistance of the falling platform, as well as any friction on the guidewires, the platform was fitted with four airjets thrusting downward. The thrust of the jets was programmed by means of a suitably designed valve. The elimination of chatter and lateral vibrations was another development task which proved quite time consuming.

Observations

A motion picture sequence, taken at 32 frames/s, is shown in Fig. 7. The fuel is benzene and the droplets have diameters of 2.0 and 2.2 mm. The center-to-center spacing is 14.5 mm. This sequence illustrates one tradeoff which has been made in the design of the experiment. The use of a single ignition spark eliminates any problems of spark timing, and minimizes the perturbations produced by the spark. However, the consequence of this design is that flame spread from one droplet to another is one of the governing phenomena.

This fact complicates the interpretation of the data. The last two frames of Fig. 7 show a single flame enveloping the two droplets. The appearance of that flame does not change and, therefore, the last frames could be used to obtain information about quasisteady flame shapes. However, if the second droplet had not ignited, the failure of a flame to spread to the neighboring droplet could not be taken as evidence that the quasisteady flames would be separate. Clearly, the transient process of flame spread from a burning droplet to an adjacent cold droplet involves many processes which are not included in the quasisteady theory.

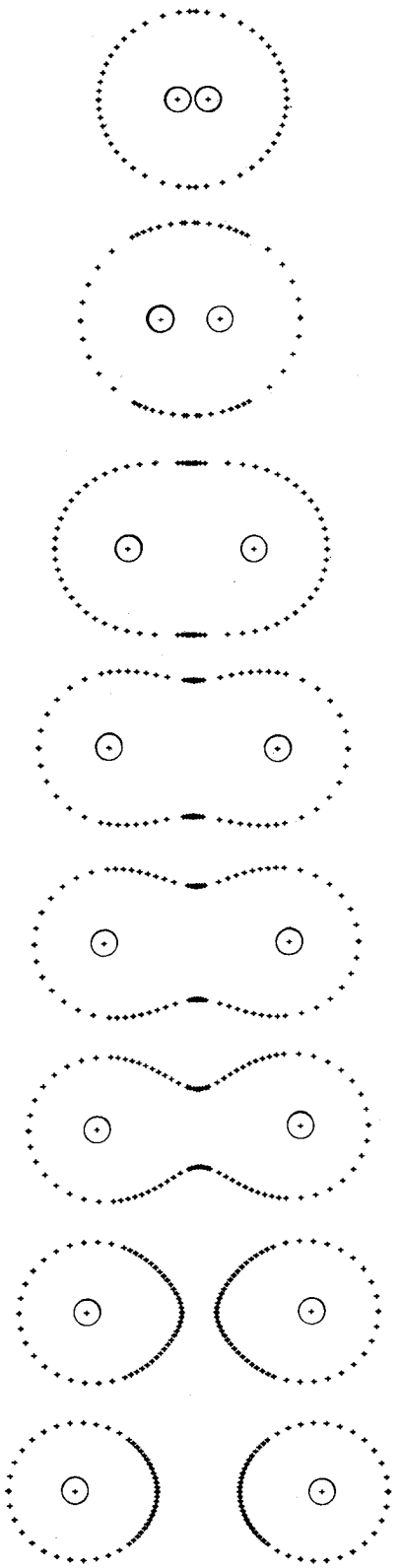

Fig. 2 Variation of flame shape with separation of equal droplets, calculated for n-heptane. Values of $2h/r$ from top to bottom: 2.40, 4.68, 10.02, 13.34, 14.68, 17.76, 19.54.

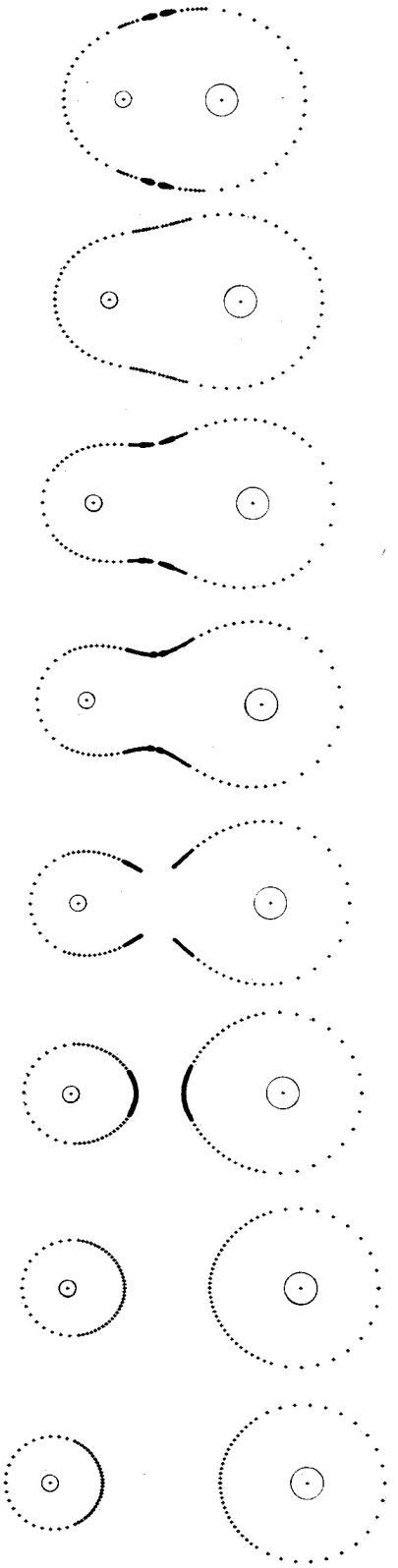

Fig. 3 Variation of flame shape with droplet separation for $r_1/r_2 = 2$, calculated for n-heptane. Values of $(h_1 + h_2)/r_2$ from top to bottom: 12.38, 16.54, 20.05, 22.07, 24.29, 26.73, 29.42, 32.37.

The dependence of flame shape on free convection is vividly shown in Fig. 8. The top figure shows a flame enveloping two benzene droplets at 0 g. The middle picture shows the asymmetry resulting from free convection at 0.005 g. The enormous asymmetry shown in the bottom frame occurs at 0.05 g.

The two photographs in Fig. 9 show a single flame enveloping two droplets of n-heptane (top) and benzene (bottom). The heptane drops have radii of 0.6 and 1.0 mm, and are located at 10.5 mm between centers. The benzene drops have radii of 1.0 and 0.7 mm, and are located at 9 mm between centers.

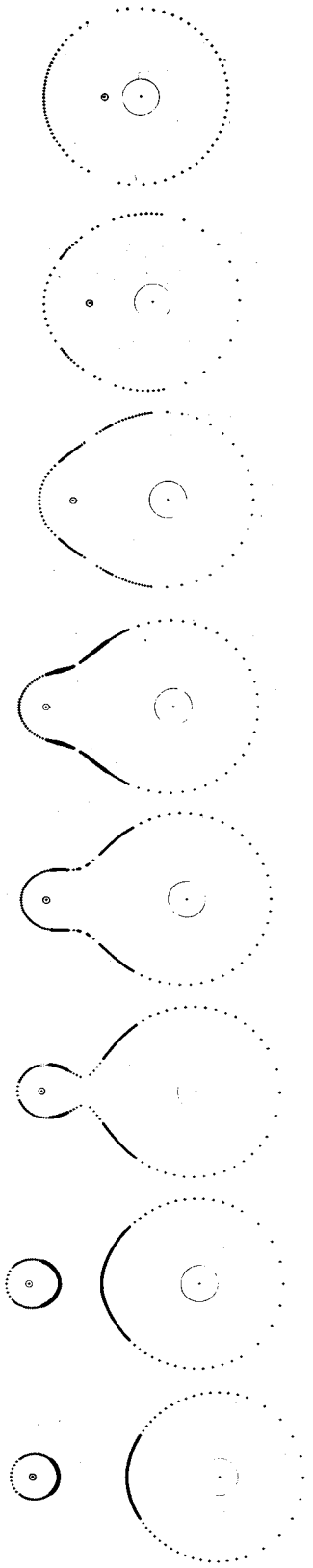

Fig. 4 Variation of flame shape with droplet separation for $r_1/r_2 = 6$, calculated for n-heptane. Values of $(h_1 + h_2)/r_2$ from top to bottom: 12.01, 20.90, 31.26, 41.92, 46.18, 50.87, 56.02, 61.69.

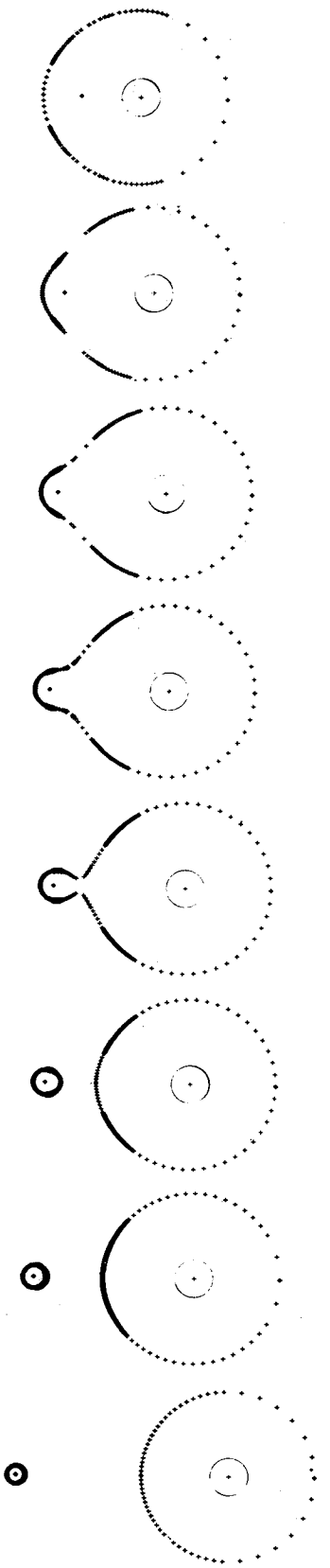

Fig. 5 Variation of flame shape with droplet separation for $r_1/r_2 = 15$, calculated for n-heptane. Values of $(h_1 + h_2)/r_2$ from top to bottom: 46.21, 69.58, 84.80, 93.52, 103.1, 113.61, 125.15, 167.08.

The dark streaks shown in the photographs of Figs. 8 and 9 are probably caused by the ignition spark. Several effects could be at work here, including electrostatic atomization of the droplet and the condensation of soot precursors on residual ions. This is an interesting phenomenon, worthy of further study.

The most obvious, and also the most significant, observation is the similarity of the flames shown in Figs. 7-9 to the computed flame shapes. It is likely, but not certain, that the outer edge of the luminous zone does indeed correspond to a flame zone, but the thickness of that flame is unknown. For

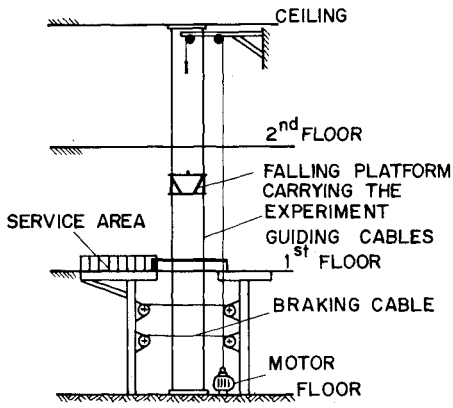

Fig. 6 Experimental facility.

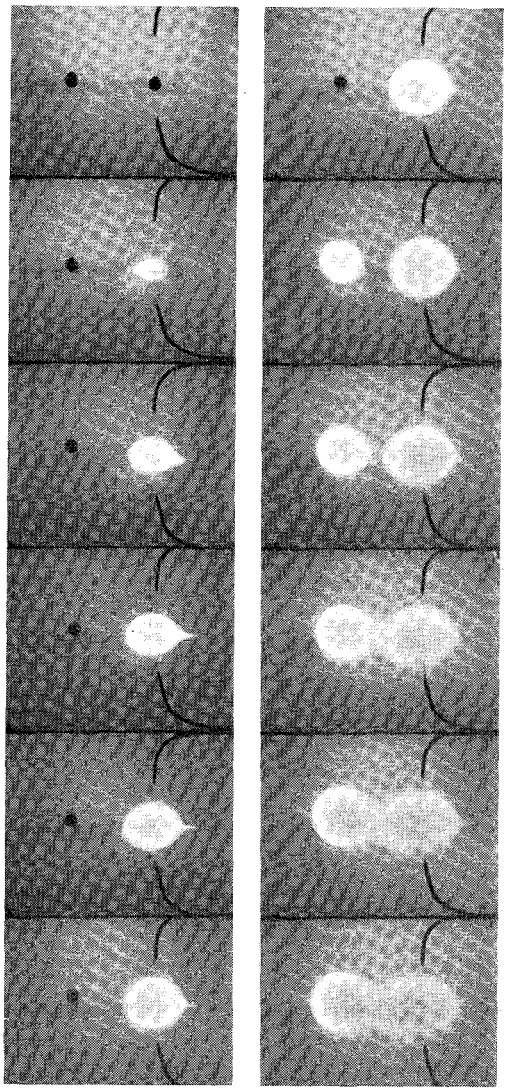

Fig. 7 Flame spread and development of quasisteady flame shape. Benzene droplets, 2.2 mm diam (left) and 2.0 mm diam (right) with $h_1 + h_2 = 14.5$ mm. Framing rate: 32 frames/s.

this reason, a detailed comparison of observed and predicted flame shapes would be far-fetched.

It is also not yet possible to obtain measurements of burning rate for comparison with theory. The droplets are necessarily large, so that their inertia might be large and the disruption caused by the withdrawal of the filaments small. They are also cold. As a result, the decrease in droplet diameter during the experimental run is small.

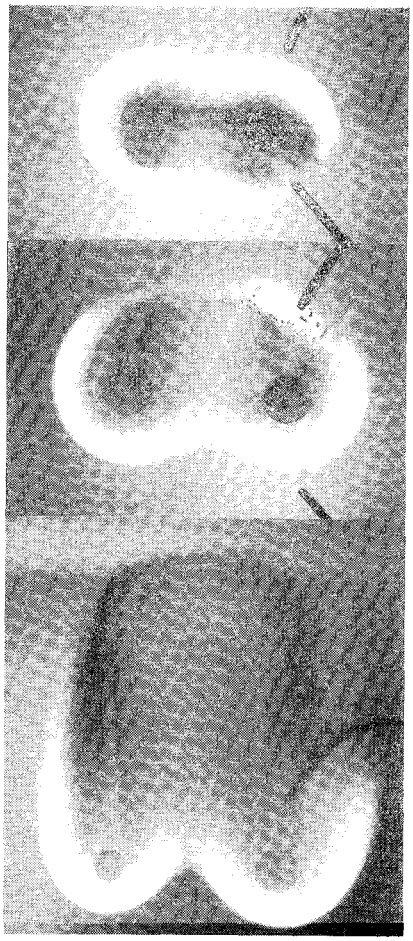

Fig. 8 Effect of g on flame shape: 0 g (top), 0.005 g (middle), 0.05 g (bottom).

All of the abovementioned features of the experiment which make it less than ideal are being addressed in current work. Nevertheless, the experiment has already shown that the essential features of the interaction between burning droplets in the absence of convection are understood.

Effect of Spacing on Burning Rate at Normal Gravity

The early experiments on the burning of fixed arrays of liquid droplets are summarized by Penner.[18] These experiments were carried out in the laboratory at normal gravity, and were, therefore, under the influence of free convection. Under these conditions it was found that the burning rate increased as the spacing between droplets decreased, reaching a maximum near the point at which the flames merged. A further decrease in separation produced a decrease in the burning rate. The explanation of this behavior, which was proposed by Penner,[18] is supported by the results of this study.

The decrease in burning rate with decreasing separation between droplets is the result of flame interaction predicted by the present analysis. In the case of combustion at normal gravity, buoyancy generated in the flame induces a flow of air over the droplet. Diffusion and heat transfer then take place through a thin boundary layer, rather than through an extensive stagnant film. As a result, the droplets must be closer together than at 0 g before their flames interact significantly.

This effect is shown in Fig. 10. The Schlieren photographs clearly show that the flames are separate in the last frame even though the equal droplets are only 6 radii apart.

To provide a maximum burning rate greater than the burning rate of the isolated droplet, two competing effects must be at play. One of them is the interaction of flames

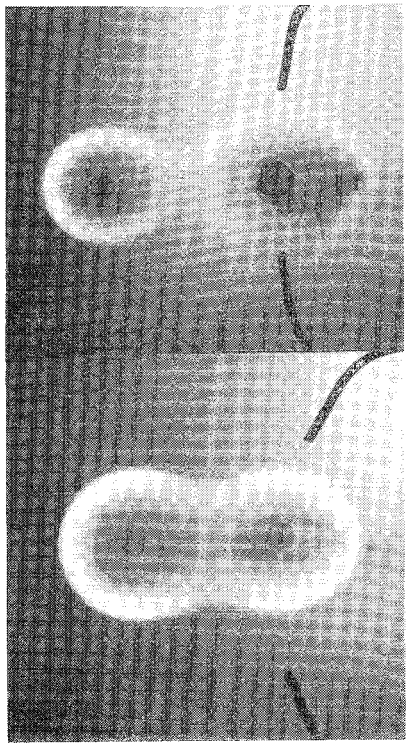

Fig. 9 Flames of pairs of droplets – top: n-heptane, radii 0.6 and 1.0 mm, $h_1+h_2=10.5$ mm; bottom: benzene, radii 1.0 and 0.7 mm, $h_1+h_2=9$ mm.

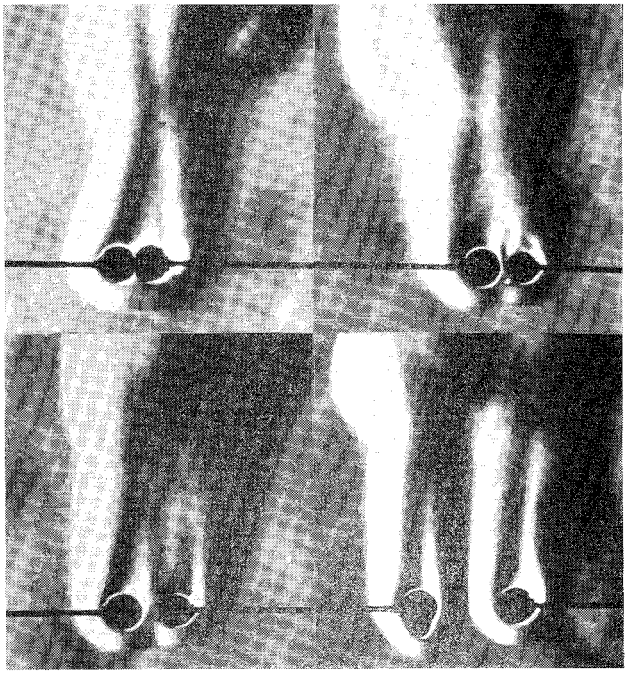

Fig. 10 Burning of two neighboring droplets of n-heptane in air at normal gravity; porous sphere experiment, sphere diam: 6 mm.

already discussed. The other is some effect which increases burning rate as the droplets approach one another. Radiation from the flame in the wake of one droplet to the wake region of the surface of the other droplet is such an effect. Luminous radiation from the trailing flame contributes a large proportion of the local heat transfer rate in that region. When the droplets are close together, but not so very close that their flames interact, this radiation could be almost twice as much as for an isolated droplet. The radiant augmentation of wake heat transfer decreases with increasing distance between droplets, tending to decrease somewhat more quickly than $1/(h_1+h_2)^2$ when the drops are far apart.

Conclusions

The analysis of the interaction between two burning droplets of arbitrary size was reduced to the solution of Laplace's equation in bispherical coordinates. It appears that the diffusion rate calculated in this way can be corrected for the effect of Stefan flow, which occurs in rapid evaporation and combustion when it is multiplied by $\ell n(1+B)$. The principal result of the analysis is the variation of the burning rates of both droplets with the spacing between them. It is noteworthy that the burning rate of the smaller droplet suffers a far greater relative reduction than that of the larger.

A free-fall experiment has provided qualitative support for the mathematical model in that the observed flame shapes of some pairs of burning droplets strongly resemble the predicted flame shapes. However, the experiment has not yet allowed a test of the predicted burning rate. It also has not allowed a test of flame shape over a wide range of droplet spacings in a way which could be interpreted without the complications of flame-spread effects. These experimental challenges remain.

A biproduct of the analysis is the important result that the thermal resistance of a small particle is increased significantly by the nearby presence of a much larger one at the same temperature. This conclusion has led to the suggestion that dust particles deposited on a warm and poorly conducting surface could ignite at a lower ambient temperature than a dilute dispersion of the same particles.

Acknowledgments

This research was sponsored in Canada by the Natural Sciences and Engineering Research Council and in Poland by the Ministry of Science, Higher Education and Technology. The contribution of J. Rapanotti in carrying out much of the computation is gratefully acknowledged.

References

[1] Chigier, N.A., "The Atomization and Burning of Liquid Fuel Sprays," *Progress in Energy and Combustion Science,* Vol. 2, 1976, pp. 97-114.

[2] Labowsky, M. and Rosner, D.E., "Conditions for Group Combustion of Droplets in Fuel Clouds: I. Quasi-steady Predictions," *Proceedings of the Symposium on the Evaporation/Combustion of Fuel Droplets,* ACS Division of Petroleum, San Francisco, Aug. 1976, (to appear in the ACS *Advances in Chemistry* series).

[3] Chiu, H.H. and Liu, T.M., "Group Combustion of Liquid Droplets," *Combustion Science and Technology,* Vol. 17, 1977, pp. 127-142.

[4] Twardus, E.M. and Brzustowski, T.A., "The Interaction Between Two Burning Fuel Droplets," *Archiwum Termodynamiki i Spalania,* Polish Academy of Science, Vol. 8, 1977, pp. 347-358.

[5] Labowsky, M., "A Formalism for Calculating the Evaporation Rates of Rapidly Evaporating Interacting Particles," *Combustion Science and Technology,* Vol. 18, 1978, pp. 145-151.

[6] Twardus, E.M. and Brzustowski, T.A., "An Experimental Study of Flame Spread and Burning in Arrays of Monosize Hydrocarbon Droplets," *Combustion Science and Technology,* Vol. 17, 1978, pp. 215-225.

[7] Sangiovanni, J.J. and Dodge, L.G., "Observations of Flame Structure in the Combustion of Monodispersed Droplet Streams," *Seventeenth Symposium (International) on Combustion,* The Combustion Institute, Pittsburgh, Pa., 1979, pp. 455-465.

[8] Moon, P. and Spencer, D.E., *Field Theory Handbook,* 2nd ed., Springer-Verlag, Berlin, 1971.

[9] Yovanovich, M.M., "A General Expression for Predicting Conduction Shape Factors," *Progress in Astronautics and Aeronautics—Thermophysics and Spacecraft Thermal Control,* edited by R.G. Hering, Vol. 35, New York, 1974, pp. 265-291.

[10] Yovanovich, M.M., *Advanced Heat Condustion,* Hemisphere Publishing Corp., Washington, 1979 (in press).

[11] Samson, R. and Deutch, J.M., "Exact Solution for the Diffusion Controlled Rate into a Pair of Reacting Sinks," *Journal of Chemical Physics,* Vol. 67, 1977, p. 847.

[12] Gradshteyn, I.S. and Ryzhik, I.W., *Table of Integrals, Series, and Products,* Academic Press, New York, 1965.

[13] Williams, F.A., *Combustion Theory,* Addison-Wesley Publshing Co., Reading, Mass., 1965.

[14] Kanury, A.M., *Introduction to Combustion Phenomena,* Gordon and Breach, New York, 1975.

[15] Kumagai, S. and Isoda, H., "Combustion of Fuel Droplets in a Falling Chamber," *Sixth Symposium (International) on Combustion,* Reinhold Publishing Corp., New York, 1957, pp. 726-731.

[16] Kumagai, S., Sakai, T., and Okajima, S., "Combustion of Free Fuel Droplets in a Freely Falling Chamber," *Thirteenth Symposium (International) on Combustion,* The Combustion Institute, Pittsburgh, Pa., 1971, pp. 779-785.

[17] Okajima, S. and Kumagai, S., "Further Investigations of Combustion of Free Droplets in a Freely Falling Chamber Including Moving Droplets," *Fifteenth Symposium (International) on Combustion,* The Combustion Institute, Pittsburgh, Pa., 1975, pp. 401-407.

[18] Penner, S.S., *Chemistry Problems in Jet Propulsion,* Pergamon Press, New York, 1957.